Hydrol. Earth Syst. Sci. Discuss., 11, 6881–6922, 2014
www.hydrol-earth-syst-sci-discuss.net/11/6881/2014/
doi:10.5194/hessd-11-6881-2014

Hydrology and Earth System Sciences Discussions

Open Access

This discussion paper is/has been under review for the journal Hydrology and Earth System Sciences (HESS). Please refer to the corresponding final paper in HESS if available.

Attribution of high resolution streamflow trends in Western Austria – an approach based on climate and discharge station data

C. Kormann[1], T. Francke[1], M. Renner[2], and A. Bronstert[1]

[1]Institute of Earth and Environmental Science, University of Potsdam, Potsdam, Germany
[2]Biospheric Theory and Modeling, Max Planck Institute for Biogeochemistry, Jena, Germany

Received: 6 June 2014 – Accepted: 16 June 2014 – Published: 26 June 2014

Correspondence to: C. Kormann (ckormann@uni-potsdam.de)

Published by Copernicus Publications on behalf of the European Geosciences Union.

Abstract

The results of streamflow trend studies are often characterised by mostly insignificant trends and inexplicable spatial patterns. In our study region, Western Austria, this applies especially for trends of annually averaged runoff. However, analysing the altitudinal aspect, we found that there is a trend gradient from high-altitude to low-altitude stations, i.e. a pattern of mostly positive annual trends at higher stations and negative ones at lower stations. At mid-altitudes, the trends are mostly insignificant. These trends were most probably caused by the following two main processes: on the one hand, melting glaciers produce excess runoff at high-altitude watersheds. On the other hand, rising temperatures potentially alter hydrological conditions in terms of less snowfall, higher infiltration, enhanced evapotranspiration etc., which in turn results in decreasing streamflow trends at low-altitude watersheds. However, these patterns are masked at mid-altitudes because the resulting positive and negative trends balance each other. To verify these theories, we attributed the detected trends to specific causes. For this purpose, we analysed the trends on a daily basis, as the causes for these changes might be restricted to a smaller temporal scale than the annual one. This allowed for the explicit determination of the exact days of year (DOY) when certain streamflow trends emerge, which were then linked with the corresponding DOYs of the trends and characteristic dates of other observed variables, e.g. the average DOY when temperature crosses the freezing point in spring. Based on these analyses, an empirical statistical model was derived that was able to simulate daily streamflow trends sufficiently well. Analyses of subdaily streamflow changes provided additional insights. Finally, it was confirmed that the main drivers of alpine streamflow changes are increased glacial melt and earlier snow melt. However, further research is needed to explicitly determine which processes related to positive temperature trends lead to the summertime streamflow decreases.

HESSD
11, 6881–6922, 2014

1 Introduction

Climate change alters the hydrological conditions in many regions (Parry et al., 2007). Especially watersheds in mountain regions are more sensitive compared to those in lowlands (Barnett et al., 2005; Viviroli et al., 2011). This is mostly due to the strong connection between mountain hydroclimatology and temperature increase, which is at least twice as strong in mountainous areas compared to the global average (Brunetti et al., 2009): on the one hand, increasing temperatures result in diminishing glaciers, earlier snowmelt and less precipitation falling in the form of snow. On the other hand, the local climate is changed by interdependencies like e.g. the snow-albedo feedback (Hall et al., 2008).

A multitude of studies have tried to assess the detailed impacts of these changes through modeling approaches. Although the credibility of observations is far stronger than that of the model results, only a few studies analyse trends in historical data. This is probably due to the fact that the aim of finding clear changing patterns is often hindered by strong noise in the data, as well as the fact that signals are usually small. A lot of trend studies in Central Europe did not find significant changes in the water cycle (cf. Pekarova et al., 2006), which has also been reported about trend studies in alpine regions (Viviroli et al., 2011).

In the European Alps, especially outside Switzerland, not much literature exists on hydrological changes in the past, although long-term and extensive datasets are available. In the mountainous areas of western North America, far more research has been carried out on changes in observational streamflow data. Many studies agree that snowmelt and thus spring freshet is appearing earlier in the year (e.g. Stewart et al., 2005; Mote et al., 2005; Knowles et al., 2006). However, most of these studies are based on indicators like “centre of volume” or “day of occurrence of the annual peak flow”, and thus should be revised: newer studies like Déry et al. (2009) and Whitfield (2013) claim that these metrics should be avoided, because they are sensitive to other factors such as record length, streamflow seasonality or data variability.

HESSD
11, 6881–6922, 2014

Apart from the changes due to earlier spring snowmelt, it is often difficult to find robust links between trend causes and their effects in observational data. Few studies have analysed the long-term effects of glacier mass loss on streamflow. Glaciers may have already reached the turning point when glacier mass has decreased to such a degree that meltwater volumes are reduced as well (Braun et al., 2000). Pellicciotti et al. (2010) showed that streamflow is still increasing in four Swiss watersheds with high glacier coverage, and decreasing in one watershed with low coverage. Stahl and Moore (2006) interpreted decreasing August streamflow in Canadian watersheds with less than 25 % glacier coverage as a sign of decreasing meltwater volumes. A representative amount of both glaciated and non-glaciated catchments and, with this, more solid and general statements would be desirable.

Next to changes through earlier snowmelt and increased glacial melt, climate change also influences streamflow through e.g. increasing evapotranspiration (Walter et al., 2004) or an increase of the timber line (Walther, 2003). However, also in this case, robust links between detected trends and their causes are missing.

In hydroclimatology, the proof that observed changes are significantly different from variations that could be explained by natural variability is referred to as *trend detection*, whereas *trend attribution* describes the assignment of these changes to specific causes. Kundzewicz (2004) underlines the importance of not only trend detection but also trend attribution to understand the reasons for these changes. In this context, it is common practice to set up comparisons or correlations between the variable under consideration and the features of the system in which it is embedded (Merz et al., 2012a). However, previous analyses usually only considered trend magnitudes as the main subject of investigation, e.g. the correlation of observed streamflow trend magnitudes with certain catchment characteristics (e.g. glacier coverage). In addition, trends used for correlation analyses were mainly derived from annual or seasonal (3-monthly) totals (e.g. Birsan et al., 2005). Both of these approaches are only partially capable of attributing trends, as streamflow integrates multiple processes across the watershed and different time scales. As a result, the isolation of single trends is often not possible, resulting in ambiguous outcomes (Merz et al., 2012a). Additionally, correlation can only give hints and does not imply causation. This is especially true in our case, as many of the watershed attributes are themselves correlated with each other (the higher a watershed, the more glaciated and the less vegetated it usually is).

Contrary to that, the present study focuses on the intraseasonal behavior of streamflow trends and compares the DOYs of the streamflow trend occurrence with trends and characteristic dates of explanatory variables such as temperature and snow height (e.g. the average DOY when spring temperature surpasses the freezing point). As additional information is gained by considering the exact temporal trend occurrence, it is possible to attribute the trends with a higher level of credibility and to further describe the link between streamflow trends and climatological catchment characteristics in a more detailed way than in previous studies. In addition, a statistical model to simulate daily streamflow trends further indicates what may be the main causes for these trends. In summary, the objectives of the present study are (1) to explain the spatially incoherent streamflow trends in Alpine regions based on annual sums; (2) to find drivers of streamflow trends in these areas, and finally (3) to attribute the streamflow trends in the study region with a high level of credibility.

The present study is a complement to Kormann et al. (2013), where 30 day moving average trends were derived for different hydroclimatic variables. Comparable to applying a moving average filter, the datasets were split into a series of 30 day average subsets and then tested for trends in all 365 days of the year. It was shown that a far more detailed picture of the changes can be obtained by daily trends than by seasonal or annual averages, where a lot of the information is lost by averaging data over a certain period of time. Furthermore, the authors stated that the timing of daily trends (i.e. the day of year when a trend turns up) potentially is a more robust measure than trend magnitude. However, similar to many other studies, the attribution of the streamflow trends in Kormann et al. (2013) was limited to interpretation only.

HESSD
11, 6881–6922, 2014

Title Page
Abstract | Introduction
Conclusions | References
Tables | Figures
◀| |▶
◀ ▶
Back | Close
Full Screen / Esc
Printer-friendly Version
Interactive Discussion

2 Data

The study area is situated in Western Austria, a relatively dry region in the rain shadow of the northern and southern Alpine border ranges. With an extent of roughly 250 km in the East–West direction and 100 km in the North–South direction, the study region includes altitudes from about 500 m up to 3700 m a.s.l. More details are given in Kormann et al. (2013). A map of the study area together with annual streamflow trends is provided in the results section (Fig. 1). In the present analysis, we studied daily observations of mean, minimum and maximum temperatures (T_{avg}: 29, T_{min}: 12 and T_{max}: 10 stations), total snow height (SH: 43 stations) and streamflow (Q: 32 gauges), which were provided by *Hydrographischer Dienst Tirol (Innsbruck), AlpS GmbH (Innsbruck), Zentralanstalt für Meteorologie und Geodynamik (Vienna)* and *Tiroler Wasserkraft AG (Innsbruck)*. T_{min} and T_{max} data was taken from the *HOMSTART* dataset (Nemec et al., 2012). Hourly temperature data was only available for the *Vernagt* station, which was provided by the *Kommission für Glaziologie* (*Munich*, Escher-Vetter et al., 2014). The IDs of the T and SH stations were generated from the rank of station height, Q station IDs from the rank of mean watershed altitude, i.e., the higher the adjacent watershed, the lower the ID. Prior to the analysis, streamflow records were normalised by catchment area (flow rate per unit area). The number of stations is a trade-off between a large number of stations that cannot be interpreted in a detailed way and an insufficient number of stations that cannot be rated as representative. The characteristics of the watersheds and their IDs are summarized in Table 1. For further information on the climatological datasets, see Kormann et al. (2013). In this paper, precipitation and snowfall were studied as well. However, as precipitation did not reveal any clear trend patterns (similar to e.g. Pellicciotti et al., 2010; Schimon et al., 2011), and snow height changes have a much stronger effect on streamflow than those of snowfall, we refrained from their further analysis. In the present study, we assume that precipitation has no trend. The validity of this assumption is supported by the fact that precipitation

HESSD
11, 6881–6922, 2014

changes are most probably of a far smaller magnitude than changes caused by e.g. increased glacial melt (see Sect. 4.2.1).

According to Kundzewicz (2004), the probability of detecting change signals increases with intensifying climate change because the impacts may be greater and persist longer. Many studies that were published e.g. in the 1990s did not have the availability of sufficient data during a phase of a strongly changing climate, as was the case since the 1980s. Only during the 30 year span between 1980 to 2010 has temperature in the Greater Alpine Region increased by about 1.3 °C, compared to about 0.7 °C between 1900 and 1980 (Auer et al., 2007). In addition, glacier mass balances have been completely negative only since the 1980s (Abermann et al., 2009). In the 1970s, there were some years with positive glacier mass balances, which could obstruct the probability of detecting a clear change signal in the hydrological time series. For these reasons and also for reasons of data availability, the present analysis was carried out for the period 1980 to 2010.

We excluded streamflow records of catchments influenced by major hydro-electric power production. Unfortunately, it was impossible to exclude all watersheds with influences from hydro power stations, as water resources in Western Austria are used extensively: only in Tirol (cf. Fig. 1), there are approximately 950 small-scale hydro power plants of differing type with a capacity lower than 10 MW[1]. However, their pondage and thus their storage volume is very limited compared to that of large dams, so we assume that the impacts on the seasonal discharge behaviour are very limited as well.

[1]http://www.kleinwasserkraft.at/en/hydropower-tyrol.

HESSD
11, 6881–6922, 2014

3 Methods

3.1 Annual analyses

3.1.1 The Mann–Kendall test and the Sen's Slope Estimator for trend detection

The rank-based Mann–Kendall (MK) test was used to calculate the trend significance. The MK test has been widely used in hydrological and climatological analyses (e.g. Gagnon and Gough, 2002; Birsan et al., 2005). Its advantages are the robustness concerning outliers, its high statistical power and the fact that it does not require a certain distribution of the data. A further description of the test is found in Hensel and Hirsch (1992).

The MK test in its original version has two main drawbacks: it accounts neither for autocorrelation in one station dataset, nor for cross-correlation between datasets of different stations. Both of them could result in the overestimation of an existent trend. Different methods of taking this into account have been published in recent years: concerning serial correlation, the prewhitening methods described in Wang and Swail (2001) were applied. Serial correlation of the data is first calculated and then removed in the case that it is higher than a certain significance level (5 % in the present case). To correct for spatial correlation in the data, a resampling approach was adopted (Livezey and Chen, 1983; Burn and Elnur, 2002): in a first step, the dataset was randomly shuffled 500 times. During this procedure, only the temporal coherence was dissolved, but not the coherence between the stations, i.e. covariance was preserved. Afterwards, all the resampled datasets were tested on trends in the same way as the original one. The percentage of stations that tested significant with a local significance level α_{local} in the original and in each of the resampled datasets was determined. A distribution of significant trends that only occurred by chance was provided by the percentage of significant results in the resampled datasets. From this distribution, the value was calculated, which was exceeded with an $\alpha_{\text{field}} = 10\,\%$ probability. This value was then compared to the percentage of significant results calculated from the original data. If

HESSD
11, 6881–6922, 2014

the percentage of significant results is higher in the original dataset, the patterns found are called "field significant".

After calculating the significance of a trend, it is necessary to estimate its magnitude, i.e. the slope of the trend. This was done by the robust linear Sen's Slope Estimator, which is computed from the mean of the slope between all possible pairs of data points (Hensel and Hirsch, 1992).

3.1.2 Minimum detectability

To cope with the problem that trends may exist but do not get detected because of a low signal-to-noise ratio, we calculated minimal detectable trends (MDT) as proposed by Morin (2011). In this publication, annual mean values and coefficients of variance were computed for global precipitation data. Monte-Carlo simulations were carried out to generate trended data with similar statistical features as the original one but with varying trends. By testing the trend significance with the Mann–Kendall test, it was possible to estimate the minimal trend that was detected as significant in 50 % of the cases. This absolute trend was named the *minimal detectable trend* for a given station at a predefined α-level. As the minimal detectable trend does not depend on the magnitude of the data, the following simplification can be derived:

$$\mathrm{MDT} = \frac{\mathrm{SNR} \cdot \sigma(X)}{\text{record length}} \tag{1}$$

SNR is the signal-to-noise ratio according to Morin (2011), and $\sigma(X)$ is the standard deviation of the series of averaged observations.

3.1.3 Fourier form models

To analyse seasonal streamflow changes, we firstly applied indicators that are able to detect a change in the timing of the seasons. We used the approach of Renner and Bernhofer (2011), where Fourier form models, which are based on harmonic functions, were fitted to the seasonal cycle of runoff. The temporal changes of these models were assessed in a following step. According to their study, the annual phase of a variable describes the timing of its maximum within a year and the amplitude describes its range. This approach was considered suitable for our purposes as well, as all of the annual hydrographs in our dataset follow a distinct seasonal cycle with strong streamflow maxima in summer and minima in winter. Fourier form models are a more robust measure than other commonly used indicators, like e.g. the centre of volume (Whitfield, 2013; Renner and Bernhofer, 2011). For further reading on this method, see Stine et al. (2009).

3.2 Seasonal analyses

3.2.1 30DMA trends and characteristic dates

To understand the relationship between streamflow trends and the variables that cause these trends, we derived high temporal resolution trends of streamflow on the one hand as the target variable and both (1) the trends and (2) characteristic dates (CD) of explanatory variables on the other hand. We assume that it is possible to represent certain processes via these trends and the CDs. If there is a temporal relationship between the streamflow trends and the trends and CDs of temperature and snow height, we suppose that this is an indicator for at least one of the causes of the Q trends.

1. Initially, high-resolution trends were derived. This approach enables the detection of finer temporal changes compared to the conventional annual or seasonal Mann–Kendall trend test. The 30 day moving average (30DMA) trends of Q, T_{mean}, T_{min} and T_{max} and SH were calculated following Kormann et al. (2013): at first, the station dataset under consideration was filtered using a 30 day moving average. The resulting time series was then tested for trends on a daily basis, considering serial and spatial correlation. The final result was a 365-value dataset per station, which provides information on whether a 30DMA trend exists for every day of the year. If this is the case, it provides the magnitude (i.e. the slope) of the trend.

HESSD
11, 6881–6922, 2014

These series allowed us to pinpoint the emergence, direction and magnitude of trends within the course of the year. In addition, daily field significances inform during which DOYs the trend patterns found were overall significant.

2. Next to the trends, characteristic dates of the seasonal cycle of Q, T_{mean}, T_{min} and T_{max} and SH were chosen. These cycles were assessed similarly to the 30DMA trends, by first calculating the mean annual cycles of the years 1980 to 2010 as 30 day moving averages for each station. Then we selected the characteristic dates: for streamflow, the DOY of the overall annual maximum streamflow ($\mathrm{DOY}_{Q_{\mathrm{max}}}$) was chosen. With regard to the CDs of T_{mean}, T_{min} and T_{max}, we selected the average DOY when temperature passes the freezing point in spring and autumn ($T = 0\,^{\circ}\mathrm{C}$ (mean DOY when $T > -0.2$ and $T < +0.2\,^{\circ}\mathrm{C}$)), as this point is crucial for multiple hydroclimatological processes in the watershed ($\mathrm{DOY}_{0^{\circ}T_{\mathrm{mean/min/max\_Spring/Autumn}}}$). Concerning snow height, the average DOY of the annual maximum snow height was chosen to indicate the date of the average start of the snowmelt in the watersheds ($\mathrm{DOY}_{\mathrm{SH}_{\mathrm{max}}}$).

The CDs of T_{mean}, T_{min} and T_{max} and SH had to be fitted to the average altitudes of the watersheds. For this purpose, the average CD of each station was depicted as a function of station height. If there was an approximate linear relationship, the DOYs of the CDs were transferred to the mean altitudes of the watersheds on the basis of a linear regression model.

3.2.2 Multiple linear model

An empirical statistical model is another tool for analysing which processes cause streamflow trends. Hence, a multiple linear model was fitted to the 30DMA streamflow trends found in the study region. This was restricted to the period between the beginning of March and mid-September (DOY 60 to DOY 250), where 85 % of the total annual streamflow and 84 % of the seasonal streamflow trends (based on absolute trend magnitudes) occur. It is approximately the time between the average annual snow height maximum (top-of-winter) in spring, before snow and glacier melt starts, and the average start of snow height increases in autumn.

Based on the previous results of this study, we gathered all possible predictor variables that could cause Q trends. Different combinations were first tested via a heuristic search based on the R-package *glmulti* (version: 1.0.7). Later, the model with the best performance in terms of an information criterion was chosen (Calcagno and de Mazancourt, 2010). Similar to the earlier analyses, all the datasets of hydroclimatological variables were filtered on the basis of 30 day moving averages. Moreover, the seasonal cycles were calculated as averages of 30 years. The $\mathrm{Trend}_{T_\mathrm{min}}$ time series are 30 DMA trends averaged over all available stations. This was feasible, as similar trends concerning timing and magnitude occur at all stations analysed.

3.2.3 Diurnal streamflow trends

To get an impression of the changes on a subdaily scale and support the previous statements based on seasonal trends, we analysed hourly streamflow and temperature data. As there were only a limited number of stations available, we selected several gauges that were representative for the area (*Gepatschalm*, *Obergurgl*, *Tumpen*; ID no. 3, 4 and 9; Table 1) with differing glacier percentages (39.3, 28.2 and 11.8 %). Obergurgl and Tumpen are both located in the Ötztal valley, Gepatschalm is located in an adjacent valley. The data was available only in the period 1985 to 2010 (compared to 1980 to 2010 for the earlier analyses). The applied methods are analogous to the previous analyses: for each station, DOY and hour, 30DMA trends were calculated and depicted in a similar way to the seasonal 30DMA trends.

HESSD
11, 6881–6922, 2014

4 Results and discussion

4.1 Trends based on annual totals/annual indicators

First, trends for annual streamflow averages were derived. These trends provide information on whether the overall yearly water yield changes, while there is no information on the seasonal water availability. Roughly two-thirds of the annual streamflow trends in the study region are not significant (Fig. 1), and no field significance was detected. The mapped trends neither depict any clear spatial trend pattern, nor show strong overall changes in Alpine hydrology. However, when presenting all the trends, both significant and insignificant, in annual streamflow totals vs. station ID – sorted by mean watershed altitude – another impression stands out (Fig. 2): it seems that high-altitude watersheds depict mostly positive trends, whereas low-altitude watersheds show negative trends. The watersheds at mid-altitudes show both positive and negative trends. Only some of the trends, where the change signal is high enough compared to the noise, are significant. The other ones are below the corresponding MDTs. This applies both for trends calculated as the percentage of annual streamflow as well as for trends derived from absolute values (Fig. 2a and b). Concerning the phase of streamflow, there is a clear signal of decreasing trends at higher stations (Fig. 2c), representing an earlier onset of spring freshet. At lower stations, phase trends are insignificant, mostly due to higher MDTs. The trends of the streamflow amplitudes show a similar behaviour to the trends of annual Q totals, but shifted to mostly negative trends (Fig. 2d): in general, amplitudes are decreasing, but less so at higher stations and more so at lower stations. The analyses of Q phase and Q amplitude confirm the different behaviour of high- and low-altitude watersheds under climate change. However, streamflow volume changes through e.g. higher glacial melt cannot be captured by the Fourier form models, as these models assume that the overall Q volume stays the same.

All the trends mentioned above show an explicit correlation with the mean watershed altitude, which does not depend on trend significance (Table 2). Note that the Pearson's correlation coefficients of significant trends are based on fewer values, so

HESSD
11, 6881–6922, 2014

in this case higher correlation coefficients are easier to obtain. All of the correlations tested significant at the $\alpha = 0.1$ level.

In summary, it seems that the processes that cause trends differ significantly from each other in higher and lower watersheds. Therefore, we derive our hypotheses as follows:

- In high-altitude, glaciated watersheds in the study region, rising temperatures result in increased glacial melt, which in turn cause positive annual streamflow trends. Most of the larger glaciers still have not reached the point where annual streamflow decreases because of decreasing glacier area.

- In low-altitude, unglaciated watersheds, increasing temperatures result in earlier snowmelt and less precipitation falling as snow. This in turn leads to multiple hydrological changes such as higher evapotranspiration, higher infiltration or changing storage characteristics, to name a few (Berghuijs et al., 2014). The negative streamflow trends in the study area are a result of these changes.

- In watersheds located at middle altitudes and covered by a smaller glacier percentage, both processes are prevalent to a lesser degree and compensate for each other. At these altitudes, trends are mostly lower than the corresponding minimal detectable trends, so in many cases, no significance is detected.

To verify these theories, it is necessary to attribute the streamflow trends. This is done via a seasonal examination of the changes, as the driving processes for these changes might be limited to a smaller scale than the annual one.

4.2 Seasonal trends

4.2.1 Trends and characteristic dates of streamflow

As already found in Kormann et al. (2013), coherent 30DMA streamflow trend patterns appear when plotted against the time of year and altitude (Fig. 3a). We refer to the

HESSD
11, 6881–6922, 2014

groups discernible in these plots as “trend patterns”. Streamflow clearly rises in spring, followed by decreases in summer; both trend patterns depend on watershed altitude. Another obvious pattern is the positive one in autumn, roughly from October to December; this one was not found to be altitude-dependent. Over most of the time, the 30DMA trends are field-significant (Fig. 3a, bar above diagram), meaning the trend patterns as a whole are statistically more frequent than expected by random chance.

At higher stations, significance of the trends calculated from annual averages was found especially where 30DMA trends in spring have high values (Fig. 3a, bar on the right). At lower stations, only two significant annual trends were detected, both at watersheds where hardly any positive 30DMA trends were detected.

The Mann–Kendall trend test has been criticised in some recent publications, particularly for the following issues: streamflow is usually not an independent and identically distributed variable, which is a precondition for using the MK test. Furthermore, a trend could be nonlinear or a part of a multispectral oscillation. Therefore, similar to Déry et al. (2009), the Sen’s Slope Estimators are presented as well without assigning trend significance (Fig. 3b). The overall results correspond to the significant ones. Furthermore, the designated patterns are even more obvious. An additional positive trend pattern appears in mid-August at higher stations, though this appears less evident than the others. Moreover, it seems that the positive Q trend signal in spring also interferes with a height-independent trend signal found during April and May to June.

We further derived the DOYs, when the annual streamflow peaks occur, averaged over 30 years: maximum Q is often found after the increasing trends in spring and before the decreasing trends in summer (Fig. 3b), which is especially true for lower stations. This means that increasing Q trends mostly occur during the rising limb, and decreasing ones during the falling limb of the seasonal hydrograph. These patterns correspond to the shift in streamflow timing to earlier DOYs.

The magnitude of the streamflow changes is very high, which supports our approach of neglecting precipitation changes when attributing the Q trends in the study region: the maximum seasonal precipitation trends found in Kormann et al. (2013) are

HESSD
11, 6881–6922, 2014

of a magnitude of about 0.15 mm $year^{-1}$, while streamflow changes reach maximum values of more than 150 mm $year^{-1}$.

4.2.2 Trends and characteristic dates of temperature and snow height

To attribute streamflow trends, one has to know the trends in other variables. Similar to the streamflow analyses, all trends are depicted, not only the significant ones.

Regarding temperature, there are differences between the T_{min}, T_{max} and T_{mean} trends, but these differences mostly concern the trend magnitude, not its direction or timing (Fig. 5a–c). Comparing single stations with each other, it is shown that the field-significant T trends appear in clusters that start and end during similar DOYs. Four main patterns of field-significant positive T trends are evident: (1) mid-March until the beginning of May, (2) mid-May until the end of June, (3) the beginning of July until mid-August, and (4) the beginning of October until mid-November. The T_{max} trends are roughly twice as intense as the ones for T_{min} and T_{mean}, but field significance was detected only in two of the four highlighted segments. For most of the stations, the magnitude and days of occurrence are similar, meaning there is no height dependence of the T trend signal. Roughly in September in T_{mean} and T_{max}, there is the only cluster of negative trends, which was similarly found by others (e.g. Nemec et al., 2012), but for the entire autumn.

Figure 5d shows the analogous results for the explanatory variable snow cover. Strong negative SH trends dominate the results; however, some positive trends occur at two high-lying stations and around November at many of the stations. Only one main cluster of field-significant trends in spring can be distinguished. Especially in snow height, it is obvious that by using the significance testing, one is not able to identify the majority of trends in the data, due to the low signal-to-noise ratio. The negative change patterns during all the winter months might exist, although no field significance was detected.

HESSD
11, 6881–6922, 2014

Besides the trends, we derived the characteristic dates of T and SH: the average DOYs of daily T_{min}, T_{max} and T_{mean} surpassing the freezing point ($DOY_{0^\circ T_{mean/max/min\_Spring/Autumn}}$) all depend on station height, in spring as well as in autumn (Fig. 4a and b, only for T_{mean}). The same applies for the average DOY of the annual snow height maximum ($DOY_{SH_{max}}$, Fig. 4c). Lines were fitted to represent these relationships. Nearly all the relationships analysed were found to be approximately linear. Only Fig. 4c shows that there might exist some height-independent $DOY_{SH_{max}}$ at mid-altitudes. However, as these irregularities were not very strong, a linear relationship was also applied. The corresponding equations were used to transfer the respective DOYs ($DOY_{0^\circ T_{mean\_Spring}}$, $DOY_{0^\circ T_{mean\_Autumn}}$, ...) to the mean altitudes of the watersheds considered in this study.

4.2.3 Comparison of the timing of trends and characteristic dates of streamflow with those of temperature and snow height

Spring ($DOY_{0^\circ T_{max\_Spring}}$ to $DOY_{0^\circ T_{min\_Spring}}$)

$DOY_{0^\circ T_{max\_Spring}}$ and $DOY_{SH_{max\_Spring}}$ appear during similar days as the first Q trends (Fig. 5e). Between $DOY_{0^\circ T_{max\_Spring}}$ and $DOY_{0^\circ T_{mean\_Spring}}$, the Q trend magnitudes further increase, most of them in shifts, i.e. first the lower basins around early March and the later ones in April. In April, there is a general major peak in the observed streamflow trends at basically all of the watersheds. This is also the time when field-significant SH trends turn up at the majority of stations (Fig. 5d). During this period, it seems that there is a height-dependent trend pattern between $DOY_{0^\circ T_{max\_Spring}}$ to $DOY_{0^\circ T_{min\_Spring}}$ superposed by a height-independent one. These ambiguous change signals are most probably caused by the following two mechanisms:

On the one hand, temperature has to overcome the 0 °C threshold to allow for snowmelt initiation. This DOY depends on the altitude of the snowpack. With T trends occurring during the same time period, $\mathrm{DOY}_{0^\circ T_{\mathrm{mean/max/min\_Spring}}}$ shifted to earlier DOYs, which probably caused the height-dependent trend pattern.

On the other hand, the average spring rise of streamflow occurs at most of the watersheds in the study region during very similar days of the year (see Kormann et al., 2013), which implies that snowmelt starts simultaneously at different altitudes. Hence, it seems that snowmelt in our study region is highly driven via weather patterns and their hydrological effects such as rain-on-snow events that influence e.g. whole valleys and not just single altitude bands. Garvelmann et al. (2014) showed that snowmelt is strongly driven via rain-on-snow events and highly depends on the previous moisture of the snow pack. With increasing T, rain-on-snow events might have turned up earlier in the season, thus causing the height-independent trend pattern during spring.

The overall strongest streamflow trends occur at high-lying watersheds after the average daily T_{mean} is positive and when T_{min} is still negative. T trends are also at their highest levels during this time of year, and the dynamics of the T trends resemble the ones in the Q trend. Pearson's r between all single streamflow trends from $\mathrm{DOY}_{0^\circ T_{\mathrm{mean\_Spring}}}$ to $\mathrm{DOY}_{0^\circ T_{\mathrm{min\_Spring}}}$ and the corresponding glacier percentage in the watershed was calculated at 0.74, which means the strongest Q trends turn up mostly at watersheds that are highly glaciated. At the uppermost catchment (ID: 1, "*Vernagt*"), constantly high positive trends of about 50 to 150 mm over the summer months are found. Compared to the average annual streamflow of 1840 mm in the years 1980 to 2010, the magnitudes of these changes can be considered dramatic. Summed up, the Q trend values over the summer roughly match the study of Braun et al. (2007): they determined the average annual glacier mass budget of the Vernagt glacier (which covers more than 70 % of watershed ID no. 1) at about -305 ± 30 mm during the years 1974 to 2005.

Some trends at mid-altitude watersheds stand out with high magnitudes and long persistence (at gauges No. 8, 12, 17). All these rivers are fed by glaciers that originate from the *Hohe Tauern* region (eastern side of the study region, cf. Fig. 1), indicating a particularly high glacial meltdown in this area. The strong Q trends at those basins

HESSD
11, 6881–6922, 2014

Attribution of HR streamflow trends in Western Austria

C. Kormann et al.

provide a further hint that these patterns are caused by glacial melt, as they still persist when the daily T_{min} has already been above 0 °C for many days.

For all these reasons, it is highly probable that the first trend pattern mentioned in this section is caused by earlier snowmelt and that the second one is a result of shrinking glaciers due to rising temperatures. However, one has to keep in mind that it is practically impossible to explicitly separate trends caused by snowmelt and those caused by glacier melt, as melt at lower glacier parts already starts while the upper parts are still covered with snow.

Summer ($DOY_{0^\circ T_{min\_Spring}}$ to $DOY_{0^\circ T_{min\_Autumn}}$)

During summer, many of the Q trends observed are negative, with the strongest ones at lower basins after T_{min} has crossed the freezing point in spring. At higher, glaciated watersheds, negative Q trends occur as soon as positive Q trends have diminished. Field significant T trends go along with these Q trends; both of them are especially strong from mid-May until mid-June. During this time of the year, the snow reservoir has already been depleted in most of the watersheds. Increasing temperatures cause increasing evapotranspiration and dryer soils. Both are further enhanced by earlier melt. At higher stations, these negative trends are balanced to a certain degree by excess water from glacial melt, evident via trends that persist longer than $DOY_{0^\circ T_{min\_Spring}}$.

Autumn ($DOY_{0^\circ T_{min\_Autumn}}$ to $DOY_{0^\circ T_{max\_Autumn}}$)

In autumn, many of the hydrographs exhibit a slightly positive trend, which does not seem to be dependent on watershed altitude. The overall trend magnitudes are far smaller than those of the spring clusters. During autumn, positive field-significant trends in T_{mean} and T_{min} were detected. $DOY_{0^\circ T_{mean\_Autumn}}$ was found during this period, but $DOY_{0^\circ T_{max\_Autumn}}$ and $DOY_{0^\circ T_{min\_Autumn}}$ do not border the Q trends as clearly as in spring. We assume that increasing T_{mean} and T_{min} during this time of year cause less snowfall and less snow to be accumulated and hence generate more rainfall-driven runoff. This generally goes along with the interpretations in earlier literature (e.g. Déry et al., 2005). As there are negative T trends in September, there is no excess glacial water to fill the gap caused by snow decreases in the previous winter, and more precipitation falling as snow in higher areas. Thus negative Q trends occur at higher, glaciated stations.

Winter (DOY$_{0^\circ T_{\mathrm{max_Autumn}}}$ to DOY$_{0^\circ T_{\mathrm{max_Spring}}}$)

All throughout winter, there is hardly any streamflow persisting in the highest watersheds. This is also reflected in the fact that there are hardly any trends at the upper 20 watersheds. Even T_{max} is below zero, so on average no melt processes are possible. The negative trends in absolute snow height were already caused at the beginning of the winter, so it is plausible that these have no effect on streamflow during mid-winter. Contrary to that, minor streamflow trends exist at lower watersheds; however, there is no clear positive or negative pattern and trend magnitudes are small. Temperatures might reach above zero in the lower catchment areas of certain watersheds, so positive Q trends could be caused through lower snow accumulation in these watersheds.

4.2.4 Empirical statistical model for the identification of streamflow trends

It was found that the best model performance is achieved with the following terms (Eq. 2). Both the response variable, the 30DMA streamflow trend (Trend$_{Q_{\mathrm{Percent}}}$), as well as the derivative of the seasonal Q cycle ($\dot{Q}_{\mathrm{avg}}$) were calculated as percentages of the long-term seasonal Q average for the DOY considered. This transformation was necessary, as the model did not otherwise sufficiently fit the extreme values.

$$\mathrm{Trend}_{Q_{\mathrm{Percent}}} = 0.17 - 9.62\,\mathrm{Trend}_{T_{\mathrm{min}}} + 0.36\frac{\Delta Q_{\mathrm{avgPercent}}}{\Delta t} + 0.59 A_{\mathrm{GlacierPercent}}\mathrm{Trend}_{T_{\mathrm{min}}} \qquad (2)$$

$\Delta Q_{\mathrm{avgPercent}}/\Delta t$ represents $\dot{Q}_{\mathrm{avg}}$ in percent, $A_{\mathrm{GlacierPercent}}$ the percentage of glaciated area in the watershed and Trend$_{T_{\mathrm{min}}}$ the 30DMA T_{min} trend in °C per year for the corresponding DOY, averaged over all stations.

The adjusted R^2 was calculated as 0.70. The large majority of the predicted trend values were in accordance with the observed ones (Fig. 6); only several very high values (> 4 %) could not be simulated well. All of these values were found at the gauge with the highest percentage of glaciated area in the watershed.

The prerequisites of a linear model (homoscedascity, normal residuals) were checked via standard diagnostic plots. Our regression approach does not presume to capture the complete set of predictors, but is just meant as an heuristic approximation, as the Durbin–Watson statistic indeed indicates. Therefore, the coefficients should be taken with caution, since standard uncertainty measures cannot be derived in that case.

The predictor $\dot{Q}_{avg}$ accounts for both positive Q trends in the rising limb of Q_{avg} (before the annual maximum) and for negative trends that turn up in the falling limb (cf. Fig. 3). Reinterpreted as a trend, $\dot{Q}_{avg}$ corresponds to a shift in an earlier streamflow timing of one day per year. As this shift is too high, the coefficient (0.36) adjusts this trend to the actual one. For the 30 year study period, this counts up to a shift of 10.8 days of earlier streamflow timing, which corresponds more or less to the literature: for example, Déry et al. (2005) found that annual peak snowmelt discharge appears roughly 8 days earlier (study period 1964–2000), Stewart et al. (2005) detected a shift of 6–19 days (1948–2003), both in North America and based on timing measures such as "centre of volume". However, depending on factors like the study period, region and the methods used, results in previous literature differ strongly. As recent studies discourage the widely used streamflow timing measures, the approach based on a regression model might stand as a possible alternative.

The predictor "$A_{Glacier}$" considers the increased excess water from glacial melt in the model. The selection of this term and not that of e.g. "decrease of glaciated area" (which has been tested as well) confirms the findings of Weber et al. (2009): as glacial melt mostly occurs at the surface, the quantity of melt water generally behaves proportionately to the extent of glaciated area in the watershed, independent of the underlying glacier thickness.

HESSD
11, 6881–6922, 2014

The glacial melt is driven via the temperature increases, hence the glacier term includes the 30DMA temperature trends. As the "$A_{\text{glacier}}\text{Trend}_{T_{\text{min}}}$" term enters the model with a positive coefficient, one can assume that the majority of the glaciers have not yet reached the point when overall streamflow decreases due to diminishing glacier mass.

The additional single term "$\text{Trend}_{T_{\text{min}}}$" has a negative coefficient, and hence accounts especially for the negative trends in summertime caused by both increased ETP and decreased snow cover accumulation.

The selection of $\text{Trend}_{T_{\text{min}}}$ instead of $\text{Trend}_{\text{Tmax}}$ is somehow surprising, as one might expect many of the streamflow trends to be strongest during daytime, when temperatures are at their highest. Indeed, the selection makes sense: the ground is potentially frozen once T_{min} falls below zero. If this is the case, additional energy is necessary for melting during daytime. With a rise in T_{min}, energy that is not needed any more for melting is now available for atmospheric warming in addition to $\text{Trend}_{T_{\text{min}}}$ alone.

The advantage that only little input data is necessary has also some drawbacks: as the model is very slim, it only captures the main factors that could cause streamflow trends in highly alpine catchments. Contributors such as changes in groundwater or precipitation are not accounted for explicitly, only via their response to the other predictors. In autumn, the model is not able to simulate the actual trends adequately either. However, these trends are small in magnitude and do not influence the overall statements too much.

4.2.5 Analysis of subdaily streamflow trends

Similar to the seasonal analyses, changes in the diurnal hydrograph were analysed by first calculating 30DMA trends and then depicting these trends according to season. However, compared to the earlier plots, the ordinate is now changed from rank of station height to hour of day. Accordingly, the averages of one day's trend magnitudes (the entire y axis) are the same values as the trend magnitudes of one station in the earlier plot.

HESSD
11, 6881–6922, 2014

The overall results of the subdaily T and Q trend analysis show similar structures to the seasonal one (Fig. 7). Concerning Q, there are certain periods when subdaily dynamics in Q trends are obvious, like the period from mid-May until mid-June. During other periods, there is hardly any difference between the trends at different times of day.

More specifically, from mid-March to early May, there is merely a diurnal dynamic in the Q trends. Positive T trends without any explicit diurnal dynamic occur at the same time. Contrasting with this, from mid-May until mid-June there is a clear dependency between the positive trends in the afternoon, the time of day and the watershed analysed: the lower the watershed and the smaller the glacier percentage, the later the Q trends occur and the lower are their magnitudes. It is probable that these trends occur for the following reasons: due to the relatively low albedo of glacial ice (~ 0.3 to 0.5) compared to snow (~ 0.7 to 0.9, Paterson, 1994), glacial melt depends stronger on incoming radiation than snowmelt. Climate change results in earlier snow-free conditions on glaciers, which in turn cause stronger glacial melt during noontime. The resulting Q trends are temporally delayed with increasing distance from the glacier. Furthermore, they are reduced with decreasing watershed altitude, probably because of the balancing effect of the negative Q trends caused by earlier snowmelt and increased ETP.

In this context, it is noteworthy that there is no clear subdaily dynamic in the negative trends during DOYs with T increases: with rising ETP, one would expect stronger negative Q reductions at noon due to the maximum necessary radiation input. This is either balanced via glacial melt or the magnitude of the changes is too small compared to the reductions due to the shift of snowmelt to earlier DOYs.

5 Summary and conclusion

The present study analyses trends and its drivers of observed streamflow time series in alpine catchments, taking data from Western Austria as example. At first, trends of annual averages were analysed: it was found that streamflow at high-altitude watersheds

HESSD
11, 6881–6922, 2014

is generally increasing, while it is decreasing overall in low-altitude watersheds. The following hypotheses are proposed: (1) positive trends at higher, glaciated watersheds are caused by increased glacial melt, (2) negative trends at lower, non-glaciated watersheds are caused by the hydrological effects of rising temperatures such as less solid precipitation (snowfall) causing higher infiltration and in particular increasing ETP, and (3) many of the trends at watersheds in mid-altitudes are not identified, because positive and negative trends cancel each other out and the final annual trend is too small to be detected. To confirm these hypotheses, we attributed the trends, i.e. we identified the processes that cause the trends.

The biggest challenge in streamflow trend attribution is that streamflow measured at one gauge integrates multiple processes all over the catchment area. This makes the identification of individual drivers difficult as the final streamflow signal is a result of multiple processes where upward and downward trends could balance each other out. The problem applies for many trend analyses in the literature, where trends are calculated from averages over a certain period of time.

Therefore, daily resolution streamflow trends are derived, as they allow for a more precise temporal localisation of the trends. The DOYs of these trends are then compared to average DOYs of other hydroclimatological characteristics, such as the temperature surpassing the average freezing point in spring, or e.g. DOYs of trends in snow height. The DOYs of these long-term characteristics fit well with the ones of the trends found in streamflow time series and thus can be related to them. Additionally, an empirical statistical model and analyses of the subdaily changes gave further hints for the causes of the streamflow changes in the study region.

In summary, we were able to attribute most of the streamflow trends especially in the first half of the year with a high level of credibility. Figures 8 and 9 present illustrations of the seasonal hydrographs for the examples of a high-altitude glaciated and a low-altitude non-glaciated watershed. Besides this, the detected trends and their probable main drivers are depicted. Our study confirms the findings of many studies in alpine regions, where drivers of streamflow changes were identified via modelling

HESSD
11, 6881–6922, 2014

approaches (e.g. Braun et al., 2010): the two main influences on alpine streamflow are the increased glacial melt and the shift to earlier snowmelt, both driven via temperature increases. We want to emphasise that our analysis is based on observed station data only. For this reason, we consider our statements concerning both the detection and the attribution of the changes to be more robust than results obtained by stand-alone model approaches. However, a few patterns still exist, where streamflow trend attribution via temperature, glacier and snow height changes is not sufficient and thus the need for further research remains: for example, we could not explicitely identify the drivers of summer streamflow decreases. Nevertheless, we found that one main reason for these reductions is the shift of snowmelt to earlier DOYs. With this, the watershed potentially receives more precipitation in the form of rain which in turn possibly leads to higher annual infiltration and interception rates. This water might be additionally available for evapotranspiration and vegetation growth and thus will reduce seasonal – and with this annual – streamflow amounts. The study of Berghuijs et al. (2014) supports this assumption for the contiguous US: they found observational evidence, that a reduction in the percentage of snow in total precipitation goes along with decreases in average streamflow.

Also higher transpiration rates through vegetation changes might be (additional) drivers of the summertime streamflow decreases: in the study area, alpine livestock farming is the main type of cultivation. The decline of this type of farming during the 1960s and 1970s (Neudorfer et al., 2012) resulted in a still ongoing overgrowth of former grasslands, enhanced by climate-change related land-use changes like increases of the timber line (Walther, 2003).

The empirical-statistical model found in the present study was proven to simulate streamflow trends sufficiently well. Not only could it serve as a tool to gain deeper insight into the processes that cause streamflow trends, but it could also be used to derive streamflow trends in such alpine catchments, where only recently a gauge has been installed. T trends were found to be quite uniform over the entire study region, so a climate station that is very close to the watershed is not absolutely mandatory. The

HESSD
11, 6881–6922, 2014

percentage of glaciated areas in the watershed can be derived via glacier cadastres or satellite imagery.

With this analysis, we have shown that the hydrological dynamics in alpine areas are changing significantly. Still, looking at the yearly averages of streamflow data, the ongoing change is masked by the fact that additional runoff caused by enhanced glacier melt and possibly increased precipitation is counter-balanced by modifications of the water cycle such as higher ETP, less snowfall and rising infiltration in the vegetation season. These opposing forces may balance out within catchments comprising higher and lower altitudes, because the increased streamflow mainly prevails in higher areas while decreasing streamflow is mostly found in lower areas. We are confident that we have identified a rather robust trend of hydrological change in specific hydro-climatological regions, e.g. alpine catchments. Even though the changes are only partially identifiable when analysing yearly averages, they can clearly be seen when studying smaller time increments. This detailed analysis of high-resolution hydrological time series follows Merz et al. (2012), who called for a more rigorous data analysis in order to analyse possible hydrological changes. The identified altered hydrological dynamics in the case of the alpine catchments is driven mostly by temperature increases. This confirms Bronstert et al. (2007) who concluded that temperature increases, rather than precipitation changes, cause hydrological changes which may be quite robustly detectable. A trend attribution of this kind is an important step towards a scientifically sound assessment of climate change impacts on hydrology. A proceeding step should be the process-based modeling of such hydrological systems (Bronstert et al., 2009), which – in case the detected trends can be replicated by the model results – can further sustain the findings concerning climate effects on alpine hydrological systems.

Our attribution approaches could possibly be applied to regions other than mountainous areas. However, one must be aware that results might be rather different and/or less well identifiable if changes are not as strongly temperature-driven as those in mountain regions. However, as stated above, hydrological trend studies should attempt to not only detect but also attribute the trends. For this reason, it is worth looking

HESSD
11, 6881–6922, 2014

for attribution methods adapted to the particular local condition. In any case, high-resolution trends are helpful, as the risk of a balancing effect between positive and negative trends is far smaller compared to trends of seasonal or annual averages.

Acknowledgements. The authors express their gratitude to *Hydrographischer Dienst Tirol (Innsbruck), AlpS GmbH (Innsbruck), Zentralanstalt für Meteorologie und Geodynamik (Vienna), Kommission für Glaziologie (Munich)* and *Tiroler Wasserkraft AG (Innsbruck)* for supplying local station data, and to Efrat Morin (Hebrew University Jerusalem, Israel) and Gerd Bürger (University of Potsdam, Germany) for inspiring discussions. This study was kindly supported by the Potsdam Research Cluster for Georisk Analysis, Environmental Change and Sustainability (PROGRESS) and the Young Scientists Exchange Program (YSEP) in the framework of German-Israeli Cooperation in Water Technology Research, both founded by the German Federal Ministry of Education and Research (BMBF). The YSEP program was additionally founded by the Ministry of Science, Technology and Space Israel (MOST).

References

Abermann, J., Lambrecht, A., Fischer, A., and Kuhn, M.: Quantifying changes and trends in glacier area and volume in the Austrian Ötztal Alps (1969–1997–2006), The Cryosphere, 3, 205–215, doi:10.5194/tc-3-205-2009, 2009.

Auer, I., Böhm, R., Jurkovic, A., Lipa, W., Orlik, A., Potzmann, R., Schöner, W., Ungersböck, M., Matulla, C., Briffa, K., Jones, P. D., Efthymiadis, D., Brunetti, M., Nanni, T., Maugeri, M., Mercalli, L., Mestre, O., Moisselin, J. M., Begert, M., Müller-Westermeier, G., Kveton, V., Bochnicek, O., Stastny, P., Lapin, M., Szalai, S., Szentimrey, T., Cegnar, T., Dolinar, M., Gajic-Capka, M., Zaninovic, K., Majstorovic, Z., and Nieplova, E.: HISTALP – Historical Instrumental Climatological Surface Time Series of the Greater Alpine Region, Int. J. Climatol., 27, 17–46, 2007.

Barnett, T. P., Adam, J. C., and Lettenmaier, D. P.: Potential impacts of a warming climate on water availability in snow-dominated regions, Nature, 438, 303–309, 2005.

Berghuijs, W. R., Woods, R. A., and Hrachowitz, M.: A precipitation shift from snow towards rain leads to a decrease in streamflow, Nat. Clim. Change Lett., doi:10.1038/nclimate2246, in press, 2014.

HESSD

11, 6881–6922, 2014

Attribution of HR streamflow trends in Western Austria

C. Kormann et al.

Birsan, M. V., Molnar, P., Pfaundler, M., and Burlando, P.: Streamflow trends in Switzerland, J. Hydrol., 314, 312–329, doi:10.1016/j.jhydrol.2005.06.008, 2005.

Burn, D. H. and Elnur, H.: Detection of hydrologic trends and variability, J. Hydrol., 255, 107–122, 2002.

Braun, L., Weber, M., and Schulz, M.: Consequences of climate change for runoff from Alpine regions, Ann. Glaciol., 31, 19–25, 2000.

Braun, L., Escher-Vetter, H., Siebers, M., and Weber, M.: Water balance of the highly glaciated Vernagt Basin, Ötztal Alps, in: The Water Balance of the Alps. Alpine space – Man & Environment, edited by: Psenner, R. and Lackner, R., Innsbruck University Press, 3, 33–42, 2007.

Bronstert, A., Kolokotronis, V., Schwandt, D., and Straub, H.: Comparison and evaluation of regional climate scenarios for hydrological impact analysis: general scheme and application example, Int. J. Climatol., 27, 1579–1594, 2007.

Bronstert, A., Kneis, D., and Bogena, H.: Interaktionen und Rückkopplungen beim hydrologischen Wandel: Relevanz und Möglichkeiten der Modellierung, Hydrol. und Wasserbewirts., 53, 289–304, 2009.

Brunetti, M., Lentini, G., Maugeri, M., Nanni, T., Auer, I., Böhm, R., and Schöner, W.: Climate variability and change in the Greater Alpine Region over the last two centuries based on multi-variable analysis, Int. J. Climatol., 29, 2197–2225, doi:10.1002/joc.1857, 2009.

Calcagno, V. and de Mazancourt, C.: glmulti an R package for easy automated model selection with (generalized) linear models, J. Stat. Softw., 34, 1–29, 2010.

Déry, S. J., Stieglitz, M., McKenna, E. C., and Wood, E. F.: Characteristics and trends of river discharge into Hudson, James, and Ungava Bays, 1964–2000, J. Climate, 18, 2540–2557, 2005.

Déry, S. J., Stahl, K., Moore, R. D., Whitfield, P. H., Menounos, B., and Burford, J. E.: Detection of runoff timing changes in pluvial, nival, and glacial rivers of western Canada, Water Resour. Res., 45, W04426, doi:10.1029/2008WR006975, 2009.

Escher-Vetter, H., Braun, L., and Siebers, M.: Hydrological and meteorological records from the Vernagtferner Basin – Vernagtbach station, for the years 2002 to 2012, doi:10.1594/PANGAEA.829530, 2014.

Gagnon, A. S. and Gough, W. A.: Hydroclimatic trends in the Hudson bay region, Canada, Can. Water Resour. J., 27, 245–262, doi:10.4296/cwrj2703245, 2002.

Garvelmann, J., Pohl, S., and Weiler, M.: Spatio-temporal controls of snowmelt and runoff generation during rain-on-snow events in a mid-latitude mountain catchment, Hydrol. Process., under review, 2014.
Hall, A., Qu, X., and Neelin, J. D.: Improving predictions of summer climate change in the United States, Geophys. Res. Lett., 35, L01702, doi:10.1029/2007GL032012, 2008.
Hensel, D. R. and Hirsch, R. M.: Statistical Methods in Water Resources, Elsevier Science, Amsterdam, 1992.
Knowles, N., Dettinger, M. D., and Cayan, D. R.: Trends in snowfall versus rainfall in the Western United States, J. Climate, 19, 4545–4559, 2006.
Kormann, C., Francke, T., and Bronstert, A.: Detection of regional climate change effects on alpine hydrology by daily resolution trend analysis in Tyrol, Austria, J. Water Clim. Change, in press, 2014.
Kundzewicz, Z. W.: Searching for changes in hydrological data, Hydrol. Sci. J., 49, 3–6, 2004.
Livezey, R. E. and Chen, W. Y.: Statistical field significance and its determination by Monte Carlo techniques, Mon. Weather Rev., 111, 46–59, 1983.
Merz, B., Maurer, T., and Kaiser, K.: Wie gut können wir vergangene und zukünftige Veränderungen des Wasserhaushalts quantifizieren?, Hydrol. Wasserbewirts., 56, 244–256, doi:10.5675/HyWa_2012,5_1, 2012a.
Merz, B., Vorogushyn, S., Uhlemann, S., Delgado, J., and Hundecha, Y.: HESS Opinions "More efforts and scientific rigour are needed to attribute trends in flood time series", Hydrol. Earth Syst. Sci., 16, 1379–1387, doi:10.5194/hess-16-1379-2012, 2012b.
Mote, P. W., Hamlet, A. F., Clark, M. P., and Lettenmaier, D. P.: Declining mountain snowpack in Western North America, B. Am. Meteorol. Soc., 86, 39–49, doi:10.1175/BAMS-86-1-39, 2005.
Morin, E.: To know what we cannot know: global mapping of minimal detectable absolute trends in annual precipitation, Water Resour. Res., 47, W07505, doi:10.1029/2010WR009798, 2011.
Nemec, J., Gruber, G., Chimani, B., and Auer, I.: Trends in extreme temperature indices in Austria based on a new homogenized dataset, Int. J. Climatol., 33, 1538–1550, doi:10.1002/joc.3532, 2012.
Neudorfer, T., Pinter, M., Kimer, L., Wendter, S., and Messner, W.: Milchwirtschaft auf Österreichs Almen – Entwicklungen und wirtschaftliche Perspektiven, BMLFUW, Vienna, 2012.
Paterson, W. S. B.: The Physics of Glaciers, 3rd Edn., Pergamon Press, Oxford, 480 pp., 1994.

Parry, M. L., Canziani, O. F., Palutikof, J. P., van der Linden, P. J., and Hanson, C. E. (Eds.) Climate Change 2007: Impacts, Adaptation and Vulnerability, Contribution of Working Group II to the Fourth Assessment Report of the Intergovernmental Panel on Climate Change, Cambridge University Press, Cambridge, 2007.
Pellicciotti, F., Bauder, A., and Parola, M.: Effect of glaciers on streamflow trends in the Swiss Alps, Water Resour. Res., 46, W10522, doi:10.1029/2009WR009039, 2010.
Pekarova, P., Miklanek, P., and Pekar, J.: Long-term trends and runoff fluctuations of European rivers, in: Demuth, S., Gustard, A., Planos, E., Scatena, F., Servat, E. (Eds.) Climate Variability and Change – Hydrological Impacts, proceedings of the 5th FRIEND World Conference. IAHS, UK; 520–525, 2006.
Renner, M. and Bernhofer, C.: Long term variability of the annual hydrological regime and sensitivity to temperature phase shifts in Saxony/Germany, Hydrol. Earth Syst. Sci., 15, 1819–1833, doi:10.5194/hess-15-1819-2011, 2011.
Schimon, W., Schöner, W., Böhm, R., Haslinger, K., Blöschl, G., Merz, R., Blaschke, A. P., Viglione, A., Parajka, J., Kroiß, H., Kreuzinger, N., and Hörhan, T.: Anpassungsstrategien an den Klimawandel für Österreichs Wasserwirtschaft, Bundesministerium für Land- und Forstwirtschaft, Umwelt und Wasserwirtschaft, Vienna, Austria, 2011.
Stahl, K. and Moore, R. D.: Influence of watershed glacier coverage on summer streamflow in British Columbia, Canada, Water Resour. Res., 42, W06201, doi:10.1029/2006WR005022, 2006.
Stewart, I., Cayan, D., and Dettinger, M.: Changes toward earlier streamflow timing across western North America, J. Climate, 18, 1136–1155, 2005.
Stine, A., Huybers, P., and Fung, I.: Changes in the phase of the annual cycle of surface temperature, Nature, 457, 435–440, 2009.
Viviroli, D., Archer, D. R., Buytaert, W., Fowler, H. J., Greenwood, G. B., Hamlet, A. F., Huang, Y., Koboltschnig, G., Litaor, M. I., López-Moreno, J. I., Lorentz, S., Schädler, B., Schreier, H., Schwaiger, K., Vuille, M., and Woods, R.: Climate change and mountain water resources: overview and recommendations for research, management and policy, Hydrol. Earth Syst. Sci., 15, 471–504, doi:10.5194/hess-15-471-2011, 2011.
Walter, M. T., Wilks, D. S., Parlange, J., and Schneider, R. L.: Increasing evapotranspiration from the conterminous United States, J. Hydrometeorol., 5, 406–408, 2004.
Walther, G.-R.: Plants in a warmer world, Perspect. Plant Ecol., 6, 169–185, 2003.

HESSD
11, 6881–6922, 2014

Weber, M., Prasch, M., Kuhn, M., Lambrecht, A., and Hagg, W.: Ice reserves – sub-project glaciology, in: Global Change Atlas, Chap. 1.8, GLOWA-Danube-Project, LMU Munich, Munich, 2009.
Weber, M., Braun, L., Mauser, W., and Prasch, M.: Contribution of rain, snow- and icemelt in the upper danube discharge today and in the future, Geogr. Fis. Din. Quat., 33, 221–230, 2010.
Whitfield, P. H.: Is "centre of volume" a robust indicator of changes in snowmelt timing?, Hydrol. Process., 27, 2691–2698, doi:10.1002/hyp.9817, 2013.
Yue, S. and Wang, C. Y.: Applicability of prewhitening to eliminate the influence of serial correlation on the Mann–Kendall test, Water Resour. Res., 38, 1068, doi:10.1029/2001WR000861, 2002.

HESSD
11, 6881–6922, 2014
Attribution of HR streamflow trends in Western Austria
C. Kormann et al.

Table 1. List of the watersheds used in this study (sorted by mean altitude) and their characteristics.

Station ID	Station name	Altitude (m)	Latitude	Longitude	Gauged Area (km^2)	Mean basin alt. (m)	Glacier coverage (%)
1	Vernagt	2640	46.8678	10.8007	11	3127	71.9
2	Vent	1891	46.8665	10.8895	90	2934	33.0
3	Gepatschalm	1895	46.9112	10.7142	55	2880	39.3
4	Obergurgl	1883	46.8717	10.9998	73	2849	28.2
5	Huben	1186	47.0508	10.9598	517	2700	15.7
6	St. Leonhard	1337	47.0796	10.8312	167	2613	15.5
7	Hinterbichl	1321	47.0026	12.3380	107	2600	14.3
8	Innergschlöß	1687	47.1099	12.4551	39	2590	29.4
9	Tumpen	924	47.1707	10.9031	786	2579	11.8
10	Ritzenried	1095	47.1329	10.7711	220	2544	13.2
11	Neukaser	1824	47.0225	11.6877	24	2499	9.6
12	Tauernhaus	1504	47.1037	12.4990	60	2474	19.4
13	Spöttling	1486	47.0106	12.6358	47	2473	10.6
14	Kühtai	1902	47.2124	10.9994	9	2448	0.0
15	Galtür-Au	1544	46.9988	10.1747	98	2411	5.7
16	Waier	931	46.9798	12.5290	285	2376	8.4
17	Sulzau	882	47.2185	12.2508	81	2354	17.2
18	Fundusalm	1600	47.1492	10.8909	13	2336	0.0
19	See i. P.	1019	47.1051	10.4541	385	2303	1.6
20	Habach	880	47.2322	12.3276	45	2117	6.9
21	Mallnitz	1174	46.9661	13.1835	85	2081	0.6
22	Steeg	1113	47.2643	10.2867	248	1951	0.0
23	Bad Hofgastein	837	47.1456	13.1184	221	1937	1.3
24	Haidbach	888	47.2377	12.4921	75	1915	0.0
25	Rauris	917	47.2233	12.9999	242	1841	1.6
26	Vorderhornbach	958	47.3842	10.5389	64	1726	0.0
27	Hopfreben	943	47.3144	10.0416	42	1701	0.0
28	Wagrain	849	47.3102	13.3112	91	1594	0.0
29	Viehhofen	861	47.3487	12.7448	151	1550	0.0
30	Mellau	673	47.3881	9.8790	229	1494	0.0
31	Laterns	830	47.2956	9.7195	33	1475	0.0
32	Ehrwald	958	47.4150	10.9159	88	1467	0.0

HESSD
11, 6881–6922, 2014

Table 2. Pearson's r between annual streamflow trends and mean watershed altitude.

	Significant trends only	Insignificant trends only	Both
Q annual, percent	0.84	0.54	0.68
Q annual, absolute	0.81	0.65	0.62
Q phase	0.86	0.68	0.83
Q amplitude	0.87	0.74	0.76

HESSD
11, 6881–6922, 2014

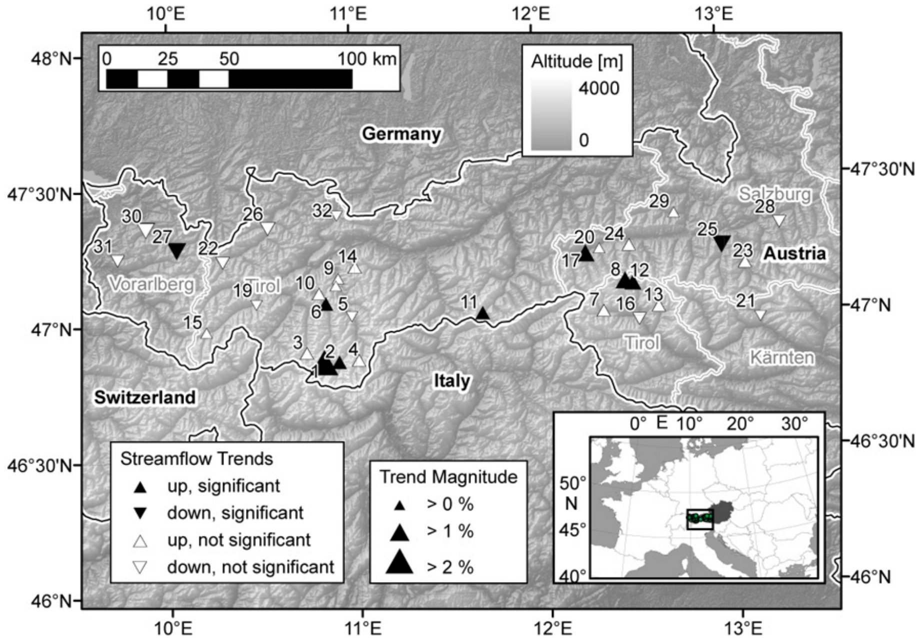

Figure 1. Study area with trends of mean annual streamflow in percent. Station ID next to the triangles.

HESSD
11, 6881–6922, 2014

Attribution of HR streamflow trends in Western Austria

C. Kormann et al.

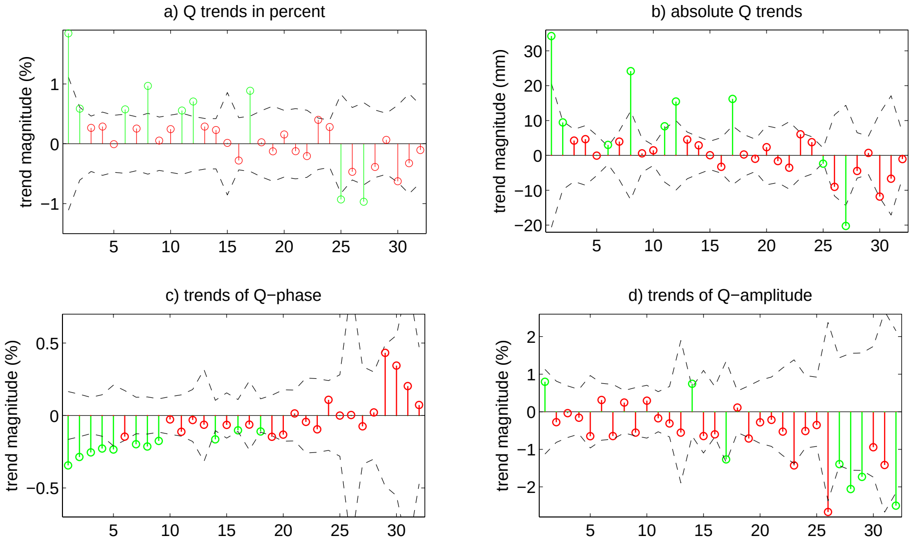

Figure 2. *x* axis: station ID sorted by mean watershed altitude (1 = highest); *y* axis: trend magnitude (percent and absolute values, resp.); grey dashes: limits of minimal detectable trends; green (red) stems: significant (insignificant) trends.

HESSD
11, 6881–6922, 2014

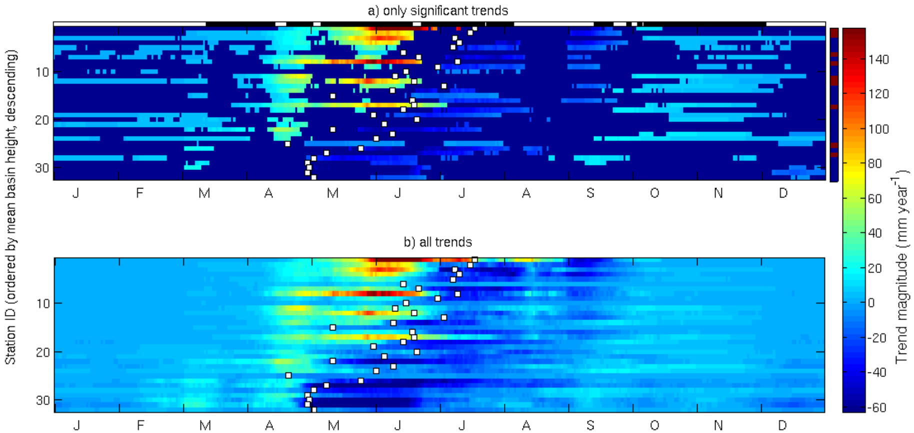

Figure 3. Annual distribution of daily streamflow trends (1980–2010); *x* axis: month; *y* axis: station ID (ordered by mean basin height, descending); *z* axis (colour): **(a)** 30DMA trend magnitude, only where significant trends are detected (dark blue if not significant); **(b)** 30DMA trend magnitude, without assigning significance; white squares: average annual *Q* maxima; bar above upper diagram: black-coloured if the 30-DMA trends are field-significant; bar on the right of upper diagram: red-coloured if the annual trend of the corresponding station is significant.

HESSD
11, 6881–6922, 2014

Attribution of HR streamflow trends in Western Austria

C. Kormann et al.

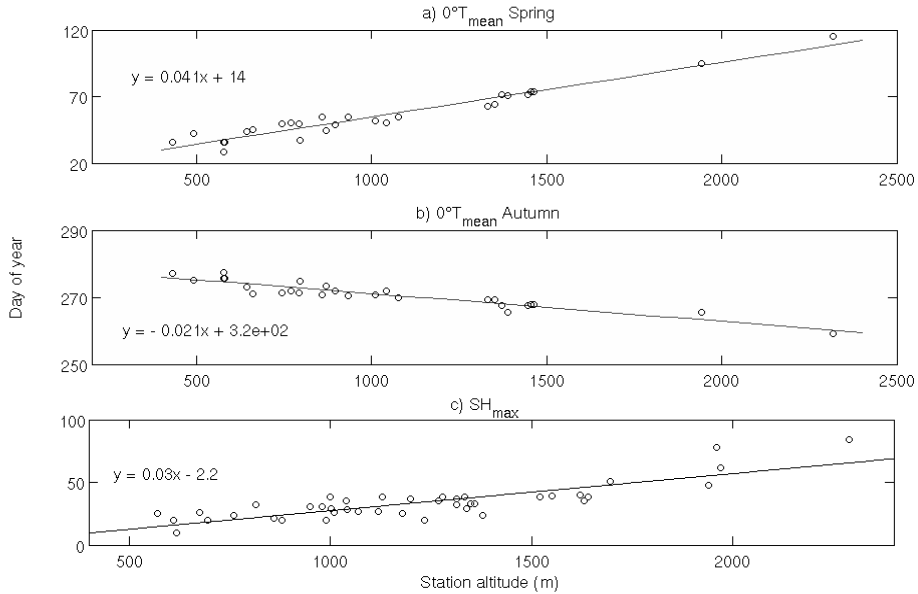

Figure 4. **(a)** Station height vs. DOY of daily T_{mean} passing the freezing point in spring; **(b)** same as **(a)**, but for autumn; **(c)** station height vs. DOY of annual SH maximum; all graphs with the line of best fit and corresponding equation. DOYs calculated as averages of the period 1980–2010.

HESSD
11, 6881–6922, 2014

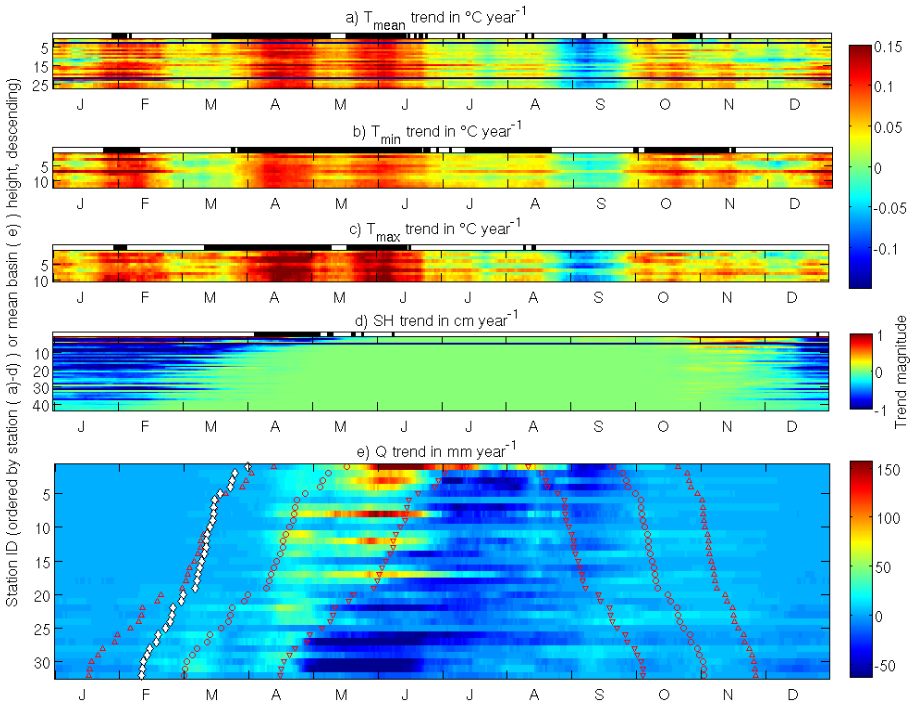

Figure 5. (a–d) Annual distribution of daily mean **(a)**, minimum **(b)** and maximum **(c)** temperature and **(d)** snow height trends (1980–2010); *x* axis: month; *y* axis: station ID (ordered by station height, descending); *z* axis (colour): 30DMA trend magnitude; bar above diagram: black-coloured if field significant. **(e)** Background: same as Fig. 3b (30DMA streamflow trends (1980–2010) without assigning significance); foreground: DOYs of the following characteristic dates depicted: **(a)** red circles (*Upward/downward triangles*): average DOY when daily mean (*maximum/minimum*) *T* passes the freezing point in spring and autumn ($DOY_{0^\circ T_{mean/max/min\_Spring/Autumn}}$); white diamonds: average DOY annual SH maximum ($DOY_{SH_{max\_Spring}}$).

HESSD
11, 6881–6922, 2014

Attribution of HR streamflow trends in Western Austria

C. Kormann et al.

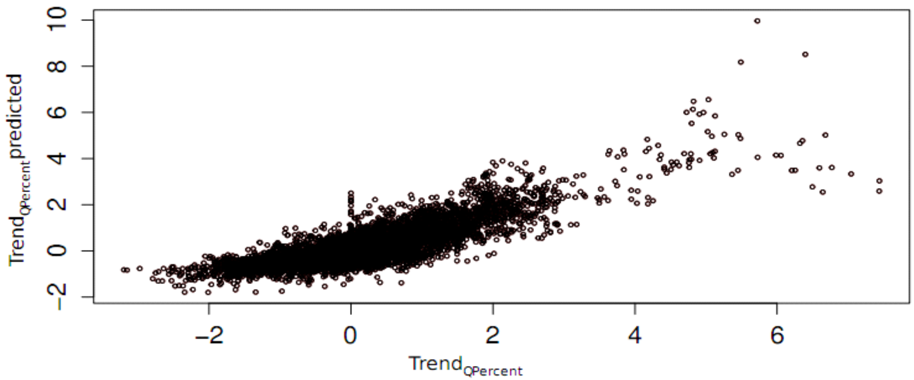

Figure 6. Scatterplot of predicted vs. observed streamflow trends in percent.

HESSD
11, 6881–6922, 2014

Attribution of HR streamflow trends in Western Austria

C. Kormann et al.

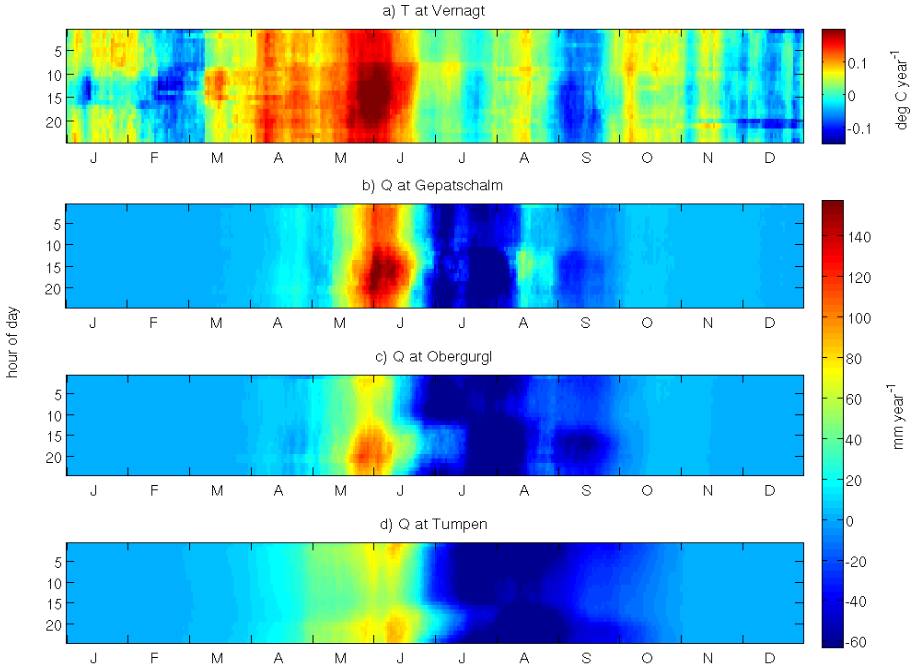

Figure 7. Daily distribution of 30DMA temperature and streamflow trends (1985–2010); *x* axis: month, *y* axis: hour of day, *z* axis: 30DMA trends in hourly resolution of **(a)** *T* at Vernagt; **(b)** *Q* at Gepatschalm; **(c)** *Q* at Obergurgl; **(d)** *Q* at Tumpen.

HESSD
11, 6881–6922, 2014

Attribution of HR streamflow trends in Western Austria

C. Kormann et al.

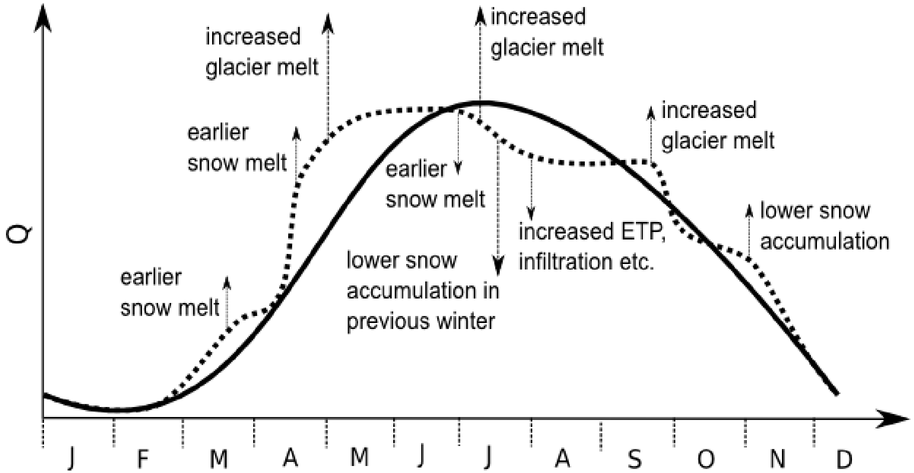

Figure 8. Simplified illustration of the original seasonal hydrograph of high-altitude, glaciated watersheds (continuous line), trends added (dashed line) and probable main drivers (period 1980–2010). Long arrows correspond to strong drivers, short arrows to smaller ones.

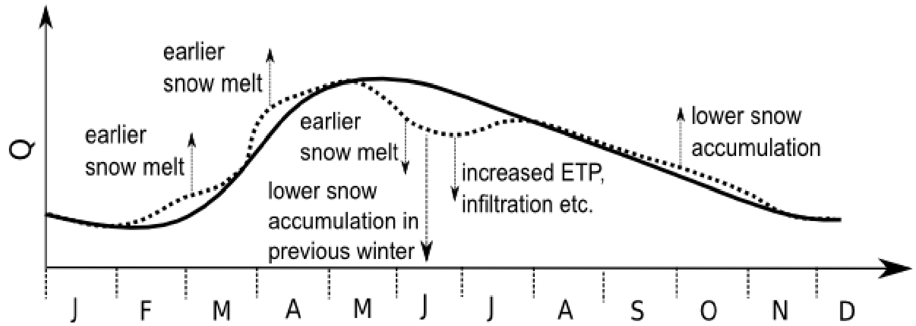

Figure 9. Similar to Fig. 8, but for low-altitude, unglaciated watersheds.

HESSD
11, 6881–6922, 2014

Attribution of HR streamflow trends in Western Austria

C. Kormann et al.

Title Page
Abstract Introduction
Conclusions References
Tables Figures
◂ ▸
Back Close
Full Screen / Esc
Printer-friendly Version
Interactive Discussion